

RANDOM CREEP AND SHRINKAGE IN STRUCTURES: SAMPLING

By Zdeněk P. Bažant,¹ F. ASCE and Kwang-Liang-Liu²

ABSTRACT: This paper deals with uncertainty in the prediction of the effects of creep and shrinkage in structures, such as deflections or stresses, caused by uncertainties in the material parameters for creep and shrinkage, including the effect of random environmental humidity. This problem was previously analyzed using two-point estimates of probability moments. Here the same problem is analyzed using latin hypercube sampling. This has the merit that the number of required deterministic structural creep analyses is reduced from 2^n to approximately $2n$, where n = number of random parameters. A method of taking into account the uncertainty due to the error of the principle of superposition is also presented. The mean and variance of creep effects in structures are calculated and scatter bands are plotted for seven typical practical examples, and the results are found to be close to those obtained with two-point estimates. Further, it is demonstrated that the distribution of creep effects is approximately normal if the creep parameters are normally distributed. Finally, it is shown that good results may also be obtained with the age-adjusted effective modulus method, which greatly simplifies structural creep analysis.

INTRODUCTION

Creep and shrinkage are the most uncertain mechanical properties of concrete. Therefore, the stochastic nature of these phenomena should be taken into account in structural analysis. Various particular aspects of the phenomena have recently been analyzed in a number of works (3,7,13,15,26), and in Ref. 19 a comprehensive yet practicable model for uncertainty analysis of creep and shrinkage effects was presented. In this model, the structural effects, such as the maximum deflection or the maximum stress, were considered as known functions of eight random parameters, $\theta_1, \dots, \theta_8$, of specified mean and variance, characterizing the uncertainties of creep compliance and material shrinkage, as well as the uncertain influences of environmental humidity and composition of concrete.

To calculate the statistics of the structural creep and shrinkage effects, the method of point estimates of probability moments was used (19). With this method, however, the computational work required becomes too great if the number n of parameters is large. Even if only two-point estimates are used, this approach requires 2^n runs of the structural analysis program, which becomes a large number ($\geq 2^{15}$) if all known stochastic parameters are considered.

The main purpose of this study is to apply another statistical method—the latin hypercube sampling, recently developed by McKay, et al. (20,21,22) and applied to a large computer code for concrete creep by

¹Prof. of Civ. Engrg. and Dir., Center for Concrete and Geomaterials, Northwestern Univ., Evanston, Ill. 60201.

²Grad. Student, Northwestern Univ., Evanston, Ill. 60201.

Note.—Discussion open until October 1, 1985. To extend the closing date one month, a written request must be filed with the ASCE Manager of Journals. The manuscript for this paper was submitted for review and possible publication on July 26, 1984. This paper is part of the *Journal of Structural Engineering*, Vol. 111, No. 5, May, 1985. ©ASCE, ISSN 0733-9445/85/0005-1113/\$01.00. Paper No. 19725.

Anderson, et al. (1,2). With this method, the number of structural analysis runs is cn where c is a constant of the order of unity. For a large number of parameters this can bring about a tremendous saving of computational work. Moreover, this method can, in general, better capture the nonlinear dependence of structural effects on the random parameters, since the entire range of statistical variation of each parameter is sampled in computations, while only a limited part of the range is sampled with the method of point estimates.

Furthermore, the sampling approach will make it possible to check whether the creep and shrinkage effects follow the normal distribution. The use of the age-adjusted effective modulus, a simplified method of creep structural analysis, will be also examined. Finally, a refinement in statistical modeling which characterizes the error of the principle of superposition will be introduced.

DETERMINISTIC CREEP AND SHRINKAGE MODEL

The deterministic creep and shrinkage model is the same as in Ref. 19, and we will outline it only briefly. The creep properties are characterized by the compliance function $J(t, t')$, which represents the strain at age t caused by a unit uniaxial stress acting since age t' . This function is taken according to the BP Model (8,9,10), which is better physically justified and has a smaller statistical error than other existing models, although it is not as simple. For the case of drying, the BP Model gives the average compliance function for the cross section. The cross section average of shrinkage strain, $\epsilon_{sh}(t, t_0)$, in which t_0 denotes the age at the start of drying, is also taken according to the BP Model.

The effects in structures are calculated on the basis of the principle of superposition expressed by the stress-strain relation

$$\epsilon(t) = \int_0^t J(t, t') d\sigma(t') + \epsilon_{sh}(t) \dots \dots \dots (1)$$

in which ϵ and σ = strain and stress. Eq. 1 is approximated by a finite sum (6,11), which makes it possible to calculate the structural effects by a step-by-step method equivalent to a series of elastic structural analyses. The solution thus obtained is nearly identical to the exact solution according to the principle of superposition.

UNCERTAINTY MODELING

One may distinguish three basic types of uncertainty: (1) The internal uncertainty, due to the random aspect of the physical mechanism of creep; (2) the external uncertainty, due to errors in the prediction of material parameters and their influencing factors, such as the environmental humidity; and (3) the error of strain measurements and environmental controls in the tests from which the material properties were ascertained.

The third type of uncertainty is not actually felt by the structure being designed; therefore, this uncertainty should be eliminated from test data and is neglected here. The first type of uncertainty should properly be treated as a random process in time (15), which is quite complicated.

However, this type of uncertainty appears to be relatively small and will therefore be neglected. Thus, only the second type of uncertainty, the external uncertainty, will be considered here.

One kind of external uncertainty is due to errors in predicting the creep compliance and the shrinkage. It may be characterized by uncertainty factors Ψ_1 , Ψ_2 and Ψ_3 , which have the mean values of 1 and are introduced as follows (19):

$$\epsilon_{sh}(t, t_0) = \Psi_1 \epsilon_{sh_2} k_h S(t, t_0) \dots \dots \dots (2)$$

$$J(t, t') = \Psi_2 \left[\frac{1}{E_0} + C_0(t, t') \right] + \Psi_3 [C_d(t, t', t_0) - C_p(t, t', t_0)] \dots \dots \dots (3)$$

in which coefficients ϵ_{sh_2} , k_h , E_0 and functions S , C_0 , C_d and C_p are defined in Ref. 8; E_0 = the instantaneous asymptotic modulus; $C_0(t, t')$ = basic creep compliance (i.e., compliance at constant moisture content); and $C_d(t, t', t_0)$ and $C_p(t, t', t_0)$ = compliance corrections due to drying.

Another kind of external uncertainty, which was not considered in Ref. 19, is due to the error of the principle of superposition (6). If the stress is strongly variable, the creep strain obtained from the principle of superposition has a greater error than if the stress is nearly constant. If the stress is constant, the principle of superposition is not needed, and then Eq. 1 reduces to $\epsilon(t) = \sigma(t_0)J(t, t_0)$. This means that an uncertainty factor, Ψ_5 , should be applied to the creep deformation in excess of this, and another uncertainty factor, Ψ_4 (no doubt of smaller variance than Ψ_5), should be applied to the subsequent elastic deformation (the mean values of Ψ_4 and Ψ_5 are also 1). Thus, we may introduce

$$\epsilon(t) = \sigma(t_0)J(t, t_0) + \int_{t_0}^t \left[\frac{\Psi_4}{E(t')} + \Psi_5 C(t, t') \right] d\sigma(t') \dots \dots \dots (4)$$

in which t_0 is the age when stress is first introduced and the first loading at t_0 is assumed to be a stress jump $\sigma(t_0)$; $E(t') = 1/J(t', t')$ = instantaneous elastic modulus at age t' ; and $C(t, t') = J(t, t') - 1/E(t')$ = creep compliance (excluding elastic deformation). The bracketed expression in Eq. 4 represents a modified compliance function.

The uncertainties due to Ψ_4 and Ψ_5 will be neglected in the present numerical examples for two reasons: (1) We want to compare the results to those of the previous study (19), in which these uncertainties were not introduced; and (2) the experimental information on Ψ_4 and Ψ_5 is too vague at present.

The remaining random parameters characterize the uncertainty in the influence of concrete composition and strength, and of environmental humidity h . In total, the following eight random parameters θ_i are considered:

$$\begin{aligned} \theta_1 &= \Psi_1; & \theta_2 &= \Psi_2; & \theta_3 &= \Psi_3; & \theta_4 &= h; \\ \theta_5 &= f'_c; & \theta_6 &= \frac{w}{c}; & \theta_7 &= \frac{g}{c}; & \theta_8 &= c \dots \dots \dots (5) \end{aligned}$$

in which c = cement content (in kilograms per cubic meter of concrete); w/c = water-cement ratio of the mix (by weight); g/c = gravel-cement

ratio (by weight); f'_c = cylindrical strength at an age of 28 days.

Note that the delay of the humidity due to diffusion of moisture between the surface and the interior points is neglected, as is the effect of humidity cycling. There are further random influencing parameters, but their influence is minor and they may be neglected. The probability distributions of parameters $\theta_1, \dots, \theta_8$ are assumed to be given.

LATIN HYPERCUBE SAMPLING

If the values of parameters $\theta_1, \dots, \theta_n$ are specified, the creep effect or response $X(\theta_i, t)$ at time t , such as the maximum deflection or the stress at a certain point, can be calculated by running a computer program for the usual deterministic creep analysis of structure. The most obvious method for determining the distribution of $X(\theta_i, t)$ is simulation (Monte Carlo method) based on random sampling of the input parameters θ_i , according to their distributions. For each randomly generated sample θ_i^k ($k = 1, 2, \dots, m$), the response X^k is calculated and the distribution of X^k may then be constructed assuming that each X^k has the same probability. This method, however, generally requires more response calculations than other methods, and also has the disadvantage that it is difficult to assess the relative importance of various input parameters θ_i .

For this reason, the method of point estimates of probability moments was employed in the previous work (19). In that method, only two values (points) $\theta_i = \bar{\theta}_i \pm s_i$, each with probability 0.5, are chosen for each input parameter ($\bar{\theta}_i$ = mean θ_i ; s_i = standard deviation of θ_i), and the response is run for all possible combinations of these input values, 2^n combinations in total. All response values then have equal probability, and one may then easily calculate the mean and variance of the response values. Moreover, the relative importance of each input parameter can be determined easily (19).

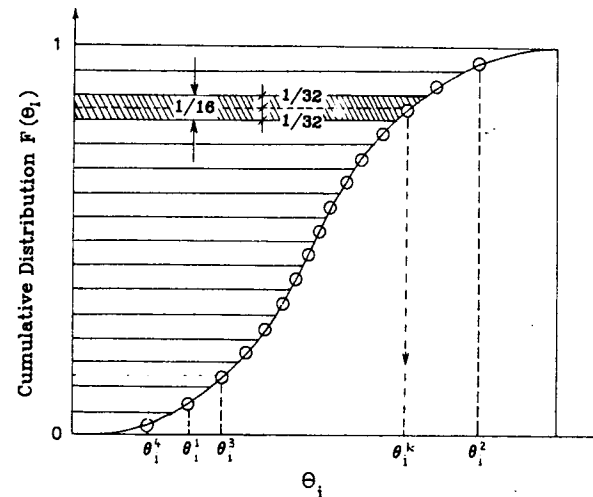


FIG. 1.—Partitioning of Range of Random Variable into Intervals

TABLE 1.—Example of Interval Numbers of Random Parameters θ_i Sampled for Individual Computer Runs (for $N = 8$)

Run (1)	θ_1 (2)	θ_2 (3)	θ_3 (4)	θ_4 (5)	θ_5 (6)	θ_6 (7)	θ_7 (8)	θ_8 (9)
1	6	2	8	6	8	3	5	1
2	1	8	5	2	3	4	7	6
3	5	6	1	3	7	2	4	8
4	4	1	7	5	6	1	8	2
5	3	4	2	1	5	7	3	5
6	2	7	3	4	1	8	5	7
7	8	5	4	7	2	6	1	4
8	7	3	6	8	4	5	2	3

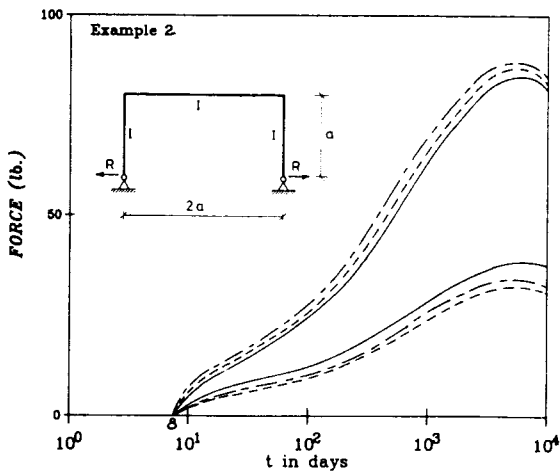
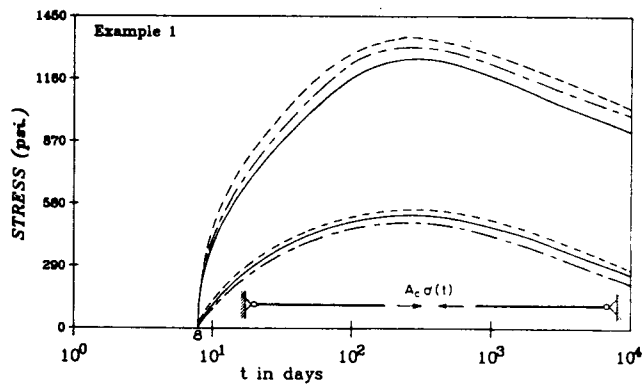


FIG. 2.—Examples of Shrinkage Stress in Restrained Bar and Shrinkage Force in Frame

A different way to diminish the number of runs is used in stratified sampling (24). Based on the known distribution $f_i(\theta_i)$ of each input parameter θ_i , the range of θ_i is partitioned into N intervals $\Delta\theta_{ik}$ (strata) of equal probability, and then m random selections of the intervals, as well as of the values within the intervals, are made.

A refinement of this approach is the Latin hypercube sampling (20,21,22). In this approach, too, the range of each parameter θ_i is partitioned into N intervals $\Delta\theta_{ik}$ ($k = 1, 2, \dots, N$) of equal probability $1/N$; see Fig. 1, in which this is sketched for cumulative normal distribution of θ_i . The number of intervals N in latin hypercube sampling is chosen to be the same as the total number of all computer runs to be made. From each interval, the parameter value is sampled exactly once, i.e., it is used in one and only one computer run. If N is large, this value need not be sampled randomly (according to the probability distribution within the interval), but may be taken at the centroid of the interval, i.e., the sampled values θ_{ik} ($k = 1, 2, \dots, N$) for a randomly selected k -value are solved from the equation $F_i(\theta_{ik}) = (k - 1/2)/N$, in which $F_i(\theta_i)$ is the cumulative distribution function of θ_i .

The special form of latin hypercube sampling used in this work consists of the following random selection of the intervals $\Delta\theta_{ik}$ to be sampled

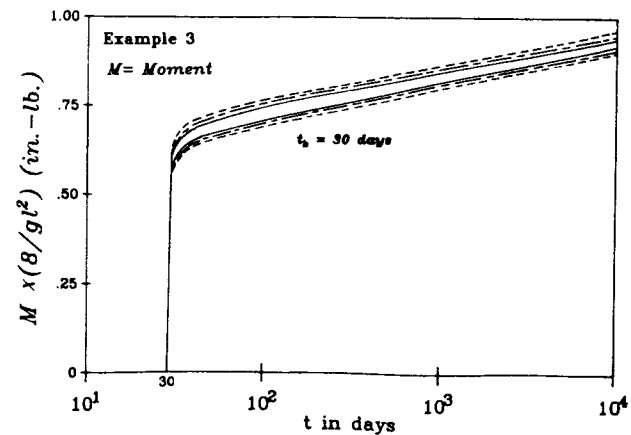
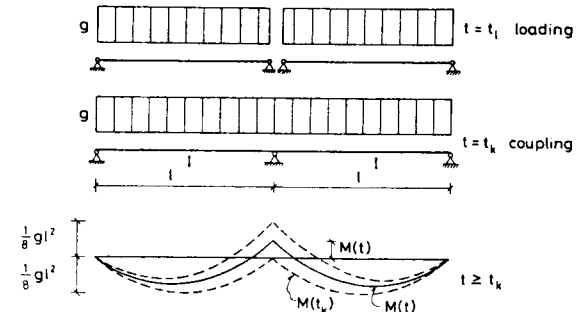


FIG. 3.—Example of Simply Supported Beam Made Continuous

for a particular computer run. With each random variable, one may associate a sequence of integers, $r_1^j, r_2^j, \dots, r_N^j$ (any one column in Table 1), representing a random permutation of the integers 1, 2, ..., N , a different random permutation for each θ_j (a standard computer library subroutine exists to generate these random permutations); see Table 1. The number k of the interval $\Delta\theta_k$ to be sampled for the input parameter θ_j for the j th computer run is then $k = r_j^j$ (e.g., according to Table 1, the sixth interval of parameter θ_2 is used for the third run). The random permutation r_1^j, \dots, r_N^j may be obtained by first generating for each θ_j a sequence of uniformly distributed integers, $u_1^j, u_2^j, \dots, u_N^j$. For each u_i^j then r_i^j may be obtained as the rank, defined as the number of all $u_i^j < u_i^j$, augmented by 1.

If the result of the j th computer run for a certain structural effect (e.g., the maximum stress at 10^4 days) is X_j , then the mean and the variance of the response may be estimated as

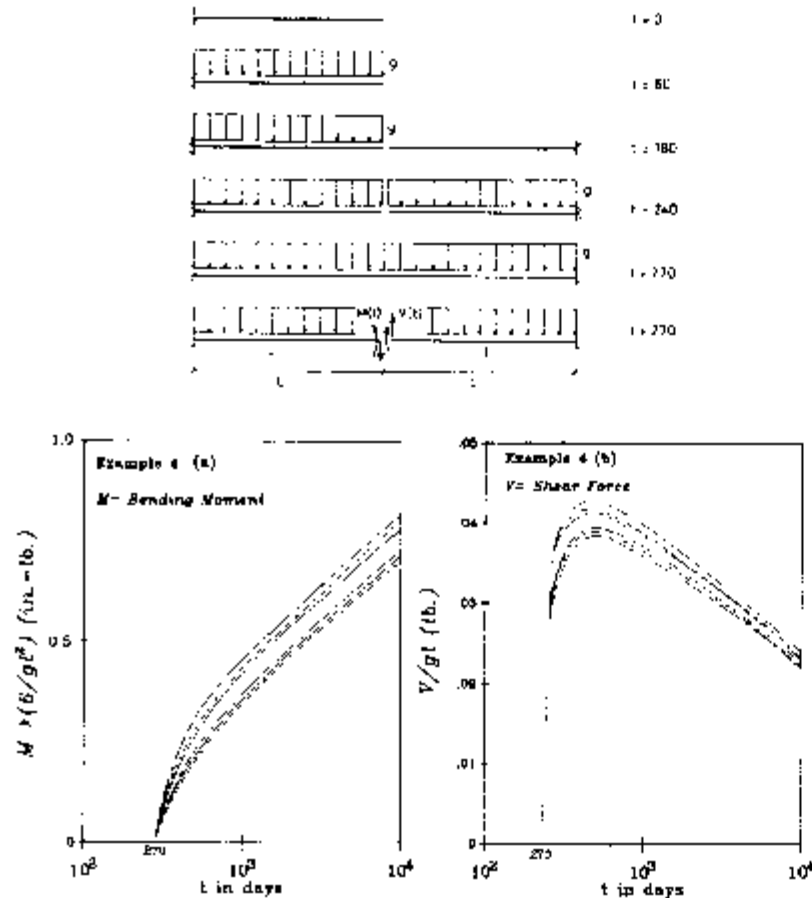


FIG. 4.—Example of Two Joined Cantilevers of Different Ages

$$\hat{X} = \frac{1}{N} \sum_{j=1}^N X_j, \quad S^2 = \frac{1}{N} \sum_{j=1}^N (X_j - \hat{X})^2 \dots \dots \dots (6)$$

These estimates are not unbiased. In fact, the unbiased estimates are not known; an unbiased estimate of X_j is not obtained as $\sum X_j / (N - 1)$. However, the unbiased estimate is between this value and $\sum X_j / N$. An estimate of $\text{Var } \hat{X}$ is known, too (21).

The latin hypercube sampling, which represents an extension of the stratified sampling (24) and the quota sampling (25), as well as a mul

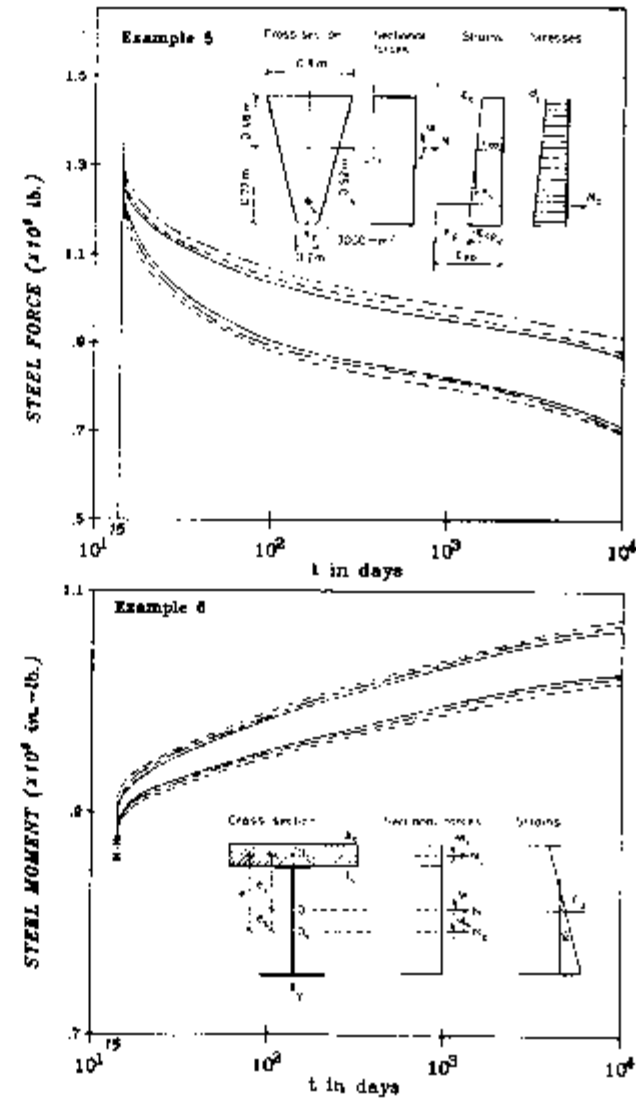


FIG. 5.—Example of Prestress Loss and of Composite Steel Concrete Beam

tidimensional generalization of the latin square sampling (14,16,17,18,24), has been shown (21,22) to give estimators (Eq. 6) of a much smaller variance than those obtained with other methods for the same number N of computer runs, provided that the response X is a *monotonic* function of parameters $\theta_1, \dots, \theta_n$ (which is usually the case for creep and shrinkage effects). Therefore, fewer computer runs are needed for the same accuracy.

Experience indicates that it usually suffices to choose $N = n$, i.e., the number of computer runs equals the number of parameters. By contrast, the method of two-point estimates of probability moments requires 2^n runs. An advantage of that method, of course, is that it allows a particularly simple assessment of the relative importance of each parameter;

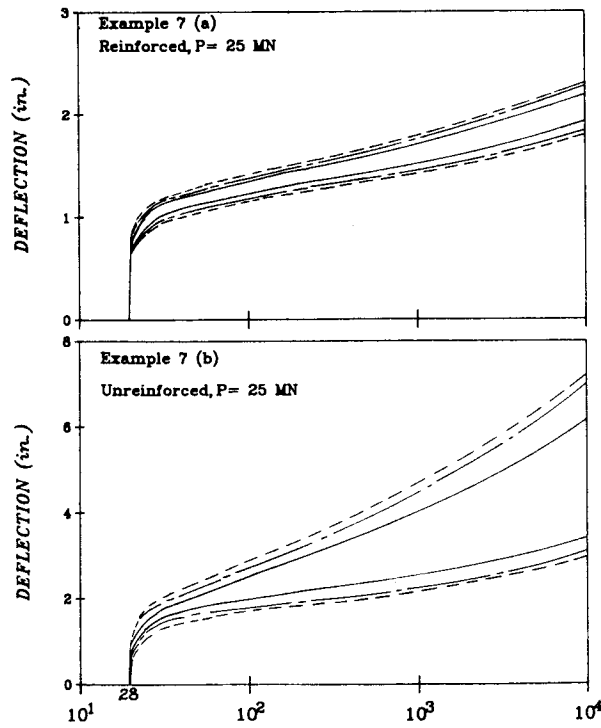
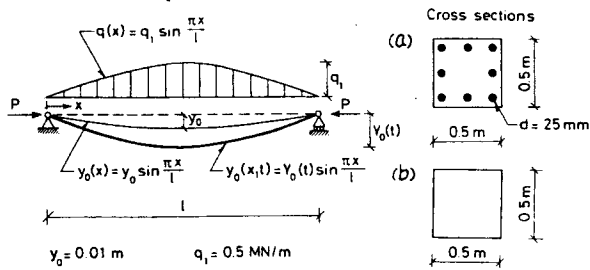


FIG. 6.—Example of Creep Buckling Deflections

for latin hypercube sampling this can also be obtained, though not as easily (20). Another advantage of the latin hypercube sampling is that the entire range of each parameter is covered, which permits better detection of nonlinear trends in the response.

NUMERICAL EXAMPLES

The use of latin hypercube sampling for uncertainty analysis of creep and shrinkage effects in structures will now be demonstrated using seven

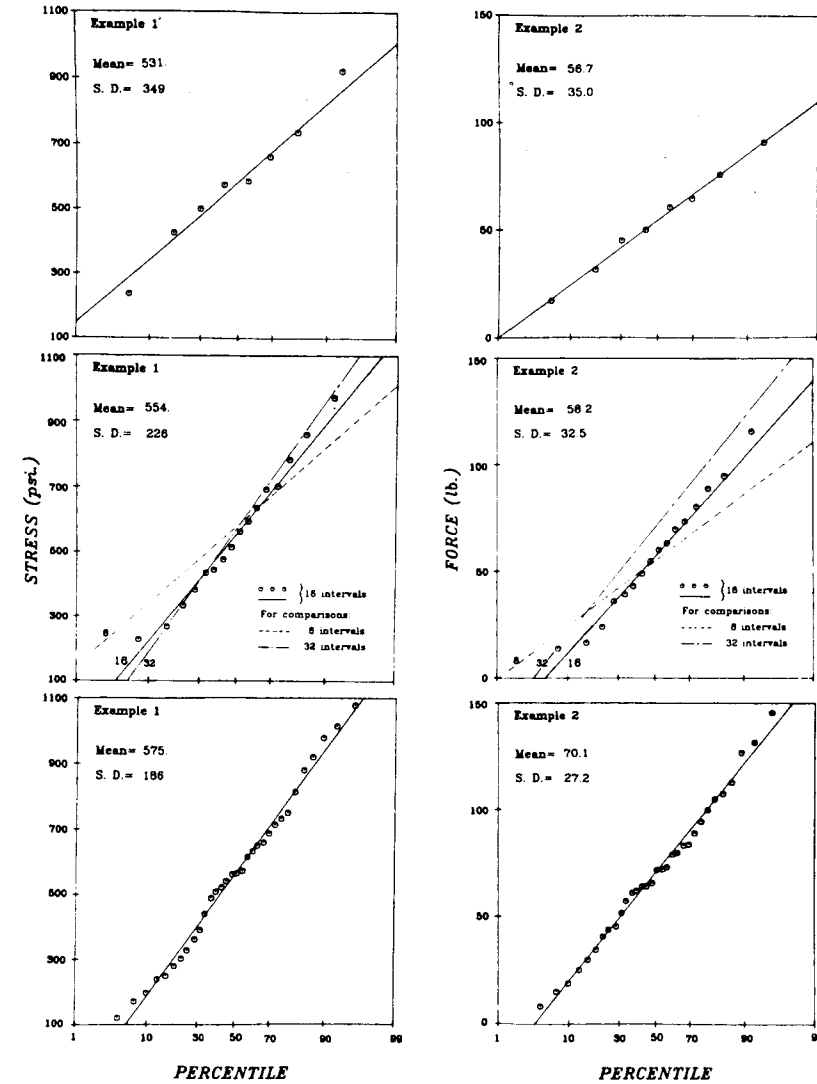


FIG. 7.—Normal Probability Plots of Results Obtained with Latin Hypercube Sampling for Examples 1 and 2

typical practical examples. These examples are the same as those solved by the method of two-point estimates in the previous work (19). Thus, it is not necessary to indicate the detailed method of structural analysis; Ref. 19 may be consulted for that.

The structures being solved in the examples are sketched in Figs. 2-6, and the curves of response versus time obtained for the examples are also plotted in Figs. 2-6; the solid lines represent $\bar{X}(t) \pm S(t)$, in which $\bar{X}(t)$ = mean response at age t , and $S(t)$ = standard deviation of the

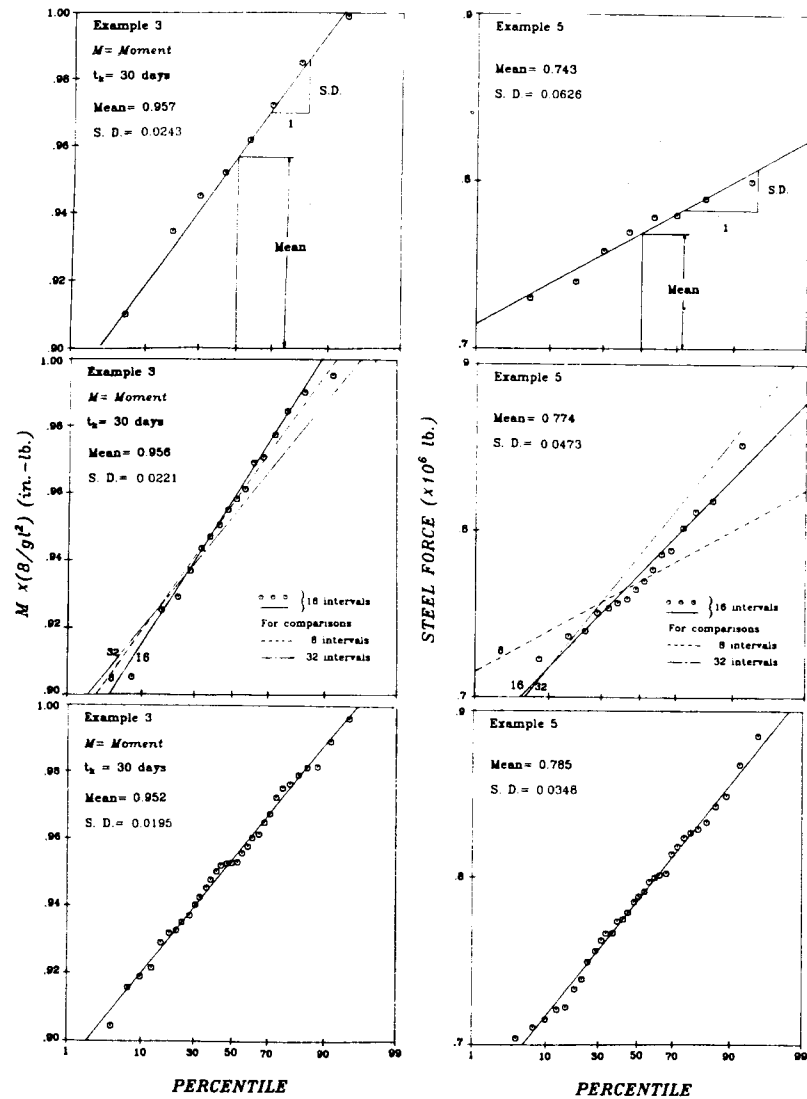


FIG. 8.—Normal Probability Plots of Results Obtained with Latin Hypercube Sampling for Examples 3 and 5

response at age t . Thus, there is a 31.74% probability that the response falls outside the band limited by these lines (15.87% above the band, 15.87% below the band). While the solid curves have been obtained with $N = 16$ (i.e., 16 subdivisions of range and 16 runs), the dash-dot lines represent cruder results obtained with $N = 8$. Finally, the dashed lines show for comparison the results obtained for the same responses in the previous work (19) by the method of two-point estimates.

Figs. 7-11 show the normal probability plots of the response values

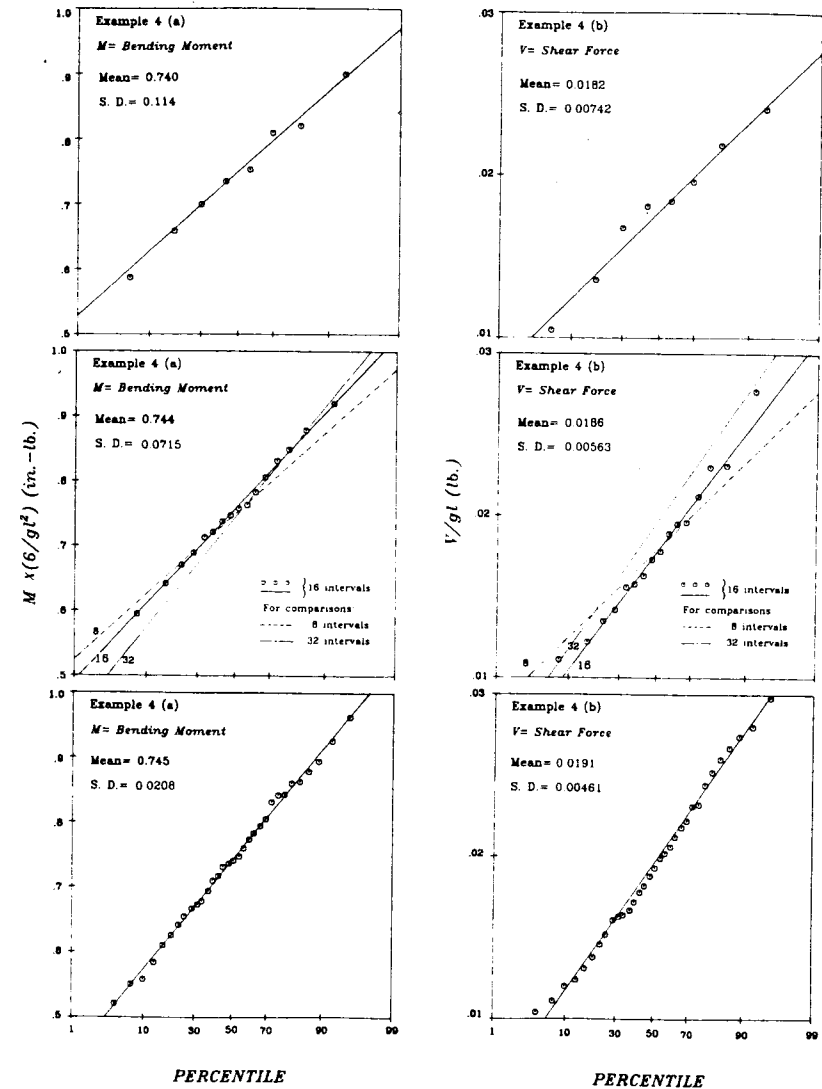


FIG. 9.—Normal Probability Plots of Results Obtained with Latin Hypercube Sampling for Example 4

obtained in the individual runs of the creep analysis program for the structure for the fixed time of $t = 10^4$ days. In these plots, for each value of X , the percentage of calculated responses of X_i less than X is plotted against X . The ordinate of the straight regression line of such a plot at 50% is the mean, and the slope of the regression line is the standard deviation. The fact that the data points (response values) in these plots fall roughly on a straight line indicates that the probability distribution of the response is approximately normal. If there were large deviations from the straight-line plots, it would mean that the normal distribution would not be a good approximation.

The normal probability plots are shown in Figs. 7–11 (for each example in three separate diagrams) for three different numbers of intervals, $N = 8, 16$ and 32 , in order to demonstrate the effect of finer partitioning of the range and of increasing the number of runs of the creep analysis program for the structure. The differences are appreciable but not large. Overall, practically acceptable accuracy in all examples is achieved with 16 subdivisions and 16 runs, i.e., $N = 2n =$ twice the number of random parameters.

For all the numerical examples, parameters $\theta_1, \dots, \theta_8$ are assumed to be normally distributed, characterized by the coefficients of variation 0.14, 0.23, 0.13, 0.2, 0.1, 0.1, 0.1 and 0.1, respectively. These values are the same for all the examples and the same as in the previous study (19). The mean values of these parameters, as well as other data and parameters for the BP Model from Ref. 8, are listed in Table 2.

For some random parameters, the partitioning of the range with a large N according to the cumulative normal distribution may give at the fringes some intervals whose centroids fall beyond physically reasonable limits of the range. For example, the centers of the marginal intervals for humidity h may fall above 1 or below 0. This is inadmissible, and a remedy would require, in a rigorous approach, abandoning the normal distribution, which would complicate analysis. As a simple, crude remedy, the tails of normal distribution outside the physical range were truncated, the remaining physical range was subdivided into N intervals of equal probability and the probability density was scaled up to give a unit area under the truncated probability distribution.

TABLE 2.—Mean Values of Parameters Used in Examples

Example (1)	Random Parameters								Other Parameters (Ref. 8)									
	Ψ_1 (2)	Ψ_2 (3)	Ψ_3 (4)	Ψ_4 (5)	Ψ_5 (6)	h (7)	f'_c (8)	w/c (9)	g/c (10)	c (11)	h_0 (12)	T (13)	D (14)	k_s (15)	a_1 (16)	s/c (17)	t_0 (18)	
1	1	1	1	1	1	0.65	45.2 ^a	0.46	2.07	450 ^a	1	23 ^b	50 ^c	1.25	1	1.66	8 ^d	
2	1	1	1	1	1	0.7	54	0.4	3.5	350	1	20	200	1.25	1	2	8	
3	1	1	1	1	1	0.65	31.5	0.6	3.0	350	1	20	400	1.1	1	2	30	
4	1	1	1	1	1	0.65	50.8	0.42	2.7	385	1	20	350	1	1	2.1	7	
5	1	1	1	1	1	0.65	54	0.4	3.0	375	1	20	345	1.2	1	2	16	
6	1	1	1	1	1	0.65	54	0.4	3.5	350	1	20	95.6	1	1	2	15	
7	1	1	1	1	1	0.65	40.5	0.5	3.4	350	1	20	250	1.2	1	2	28	

^aIn kilograms per cubic meter of concrete.

^bIn degrees Celsius.

^cIn millimeters.

^dIn days.

^eIn megapascals (mean f'_c is calculated from w/c using Bolomey's formula as in Ref. 19).

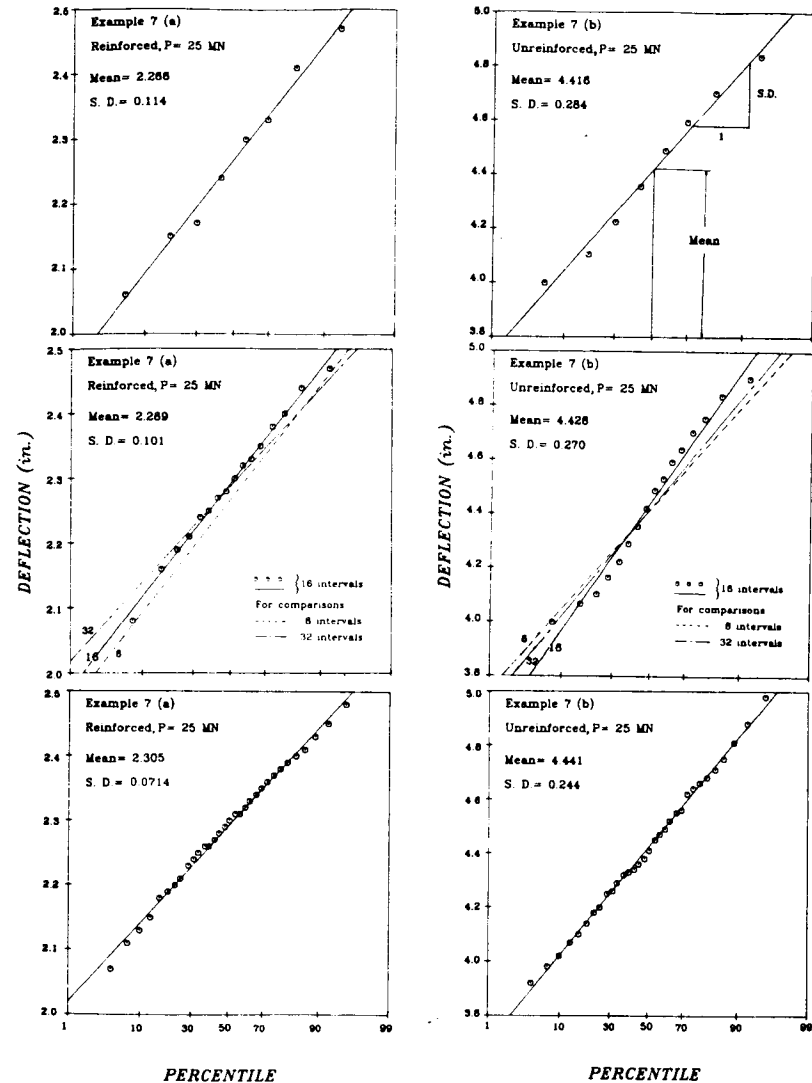


FIG. 10.—Normal Probability Plots of Results Obtained with Latin Hypercube Sampling for Example 7

The examples are further specified by the following data.

1. Shrinkage Stress in a Restrained Bar (Figs. 2 and 7)—Unreinforced bar; no cracking assumed.
2. Reaction Due to Restrained Shrinkage in a Frame (Figs. 2 and 7)— $a = 5$ m; $I = 0.00213$ m⁴.
3. Simply Supported Beams Made Continuous (Figs. 3 and 8)— $t_k = 30$ or 100 days = ages when the beams are joined; $t_1 = 30$ days = age at which

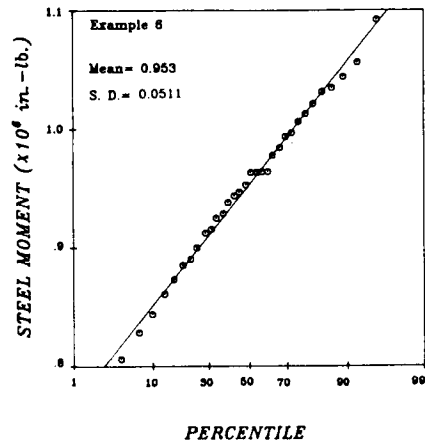
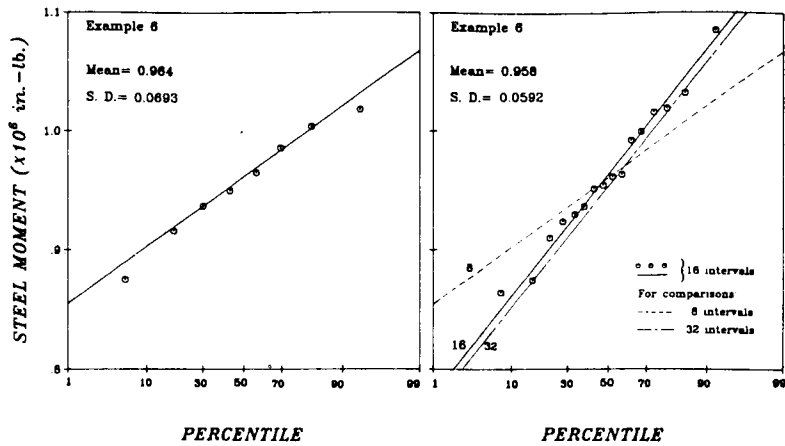


FIG. 11.—Normal Probability Plots of Results Obtained with Latin Hypercube Sampling for Example 6

the beams are assumed to start carrying the dead load.

4. *Coupling of Cantilevers of Different Ages* (Figs. 4 and 9)—Construction sequence in Fig. 4, with times given in days; uniform moment of inertia I .

5. *Prestress Loss in a Prestressed Concrete Beam* (Figs. 5 and 8).—Tendon cross section $A_s = 30 \text{ cm}^2$; eccentricity $y_p = 52 \text{ cm}$; steel with $E_p = 200,000 \text{ MPa}$ ($29 \times 10^6 \text{ psi}$); concrete cross section with area 0.6 m^2 (930 sq in.) and $I_c = 63.36 \times 10^{-3} \text{ m}^4$ ($152,000 \text{ in.}^4$); prestress strain $\epsilon_{pp} = 6 \times 10^{-3}$ (bonded reinforcement); applied bending moment $M = 1 \text{ MNm}$ ($8,851 \text{ kip} \times \text{in.}$), with no applied axial force.

6. *Stress Redistribution in Steel-Concrete Composite Beam* (Figs. 5 and 11)—Applied bending moment $M = 284 \text{ kNm}$ ($8,851 \text{ kip} \times \text{in.}$), with no applied axial force; concrete cross section $A_c = 1,650 \text{ cm}^2$ (225.1 sq in.) and $I_c = 14,210 \text{ cm}^4$ (341.4 in.^4) about its centroid; steel cross section $A_s =$

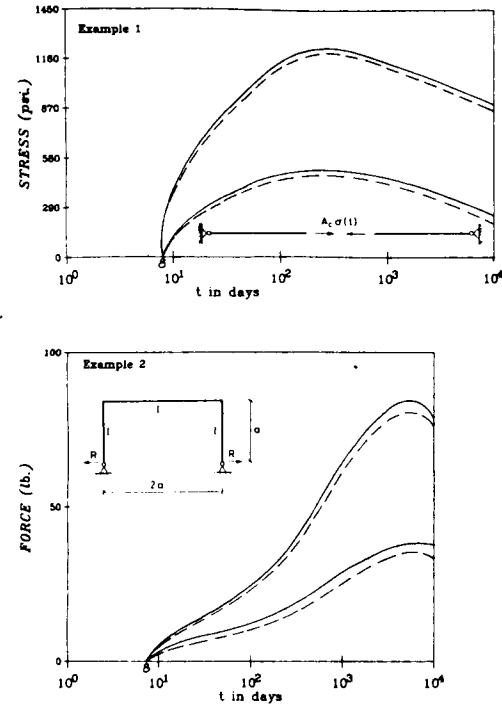


FIG. 12.—Examples 1 and 2 (Same as Fig. 2), by Age-Adjusted Effective Modulus

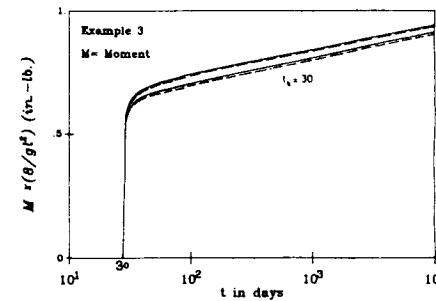
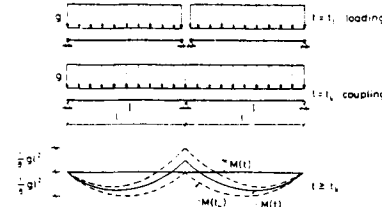


FIG. 13.—Example 3 (Same as Fig. 3), by Age-Adjusted Effective Modulus

94.9 cm² (14.71 sq in.); $I_s = 33,300 \text{ cm}^4$ (800 in.⁴) about its centroid; $e = 27.9 \text{ cm}$ (10.98 in.) = distance between centroids of steel and concrete; steel modulus $E_s = 210,000 \text{ MPa}$ ($30.46 \times 10^6 \text{ psi}$).

7. Creep Buckling Deflections (Fig. 6–10)—Pin-ended column with sinusoidal initial curvature.

In general, we see in Figs. 2–6 a relatively good agreement with the results obtained previously by two-point estimates. Where the difference is more significant, the present result is probably more accurate, especially if N is large.

APPLICATION OF AGE-ADJUSTED EFFECTIVE MODULUS

This simplified method, included in the current ACI Recommendation (23), is based on a rigorous theorem (5) which states that if the strain varies linearly with the compliance function $J(t, t')$, then the stress varies linearly with the relaxation function $R(t, t')$. Based on this property, the following algebraic quasi-elastic stress-strain relation may be derived (5, 12):

$$\Delta\epsilon(t) = \Psi_4 \frac{\Delta\sigma(t)}{E''(t, t_0)} + \frac{\sigma(t_0)}{E(t_0)} \phi(t, t_0) + \Delta\epsilon_{sh}(t) \dots \dots \dots (7)$$

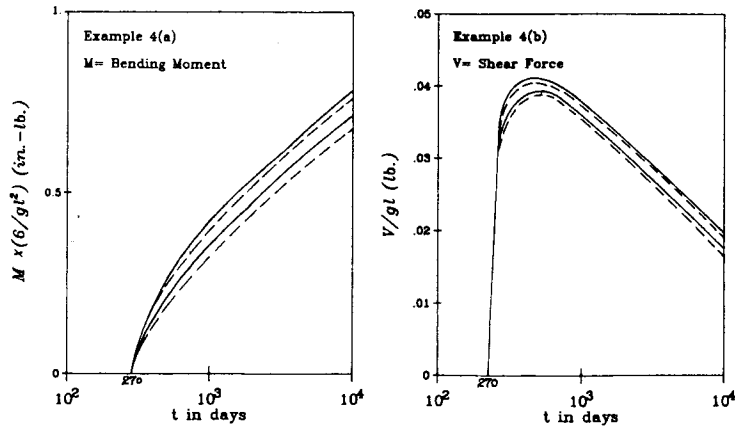
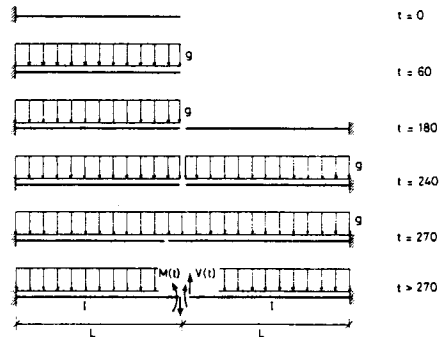


FIG. 14.—Example 4 (Same as Fig. 4), by Age-Adjusted Effective Modulus

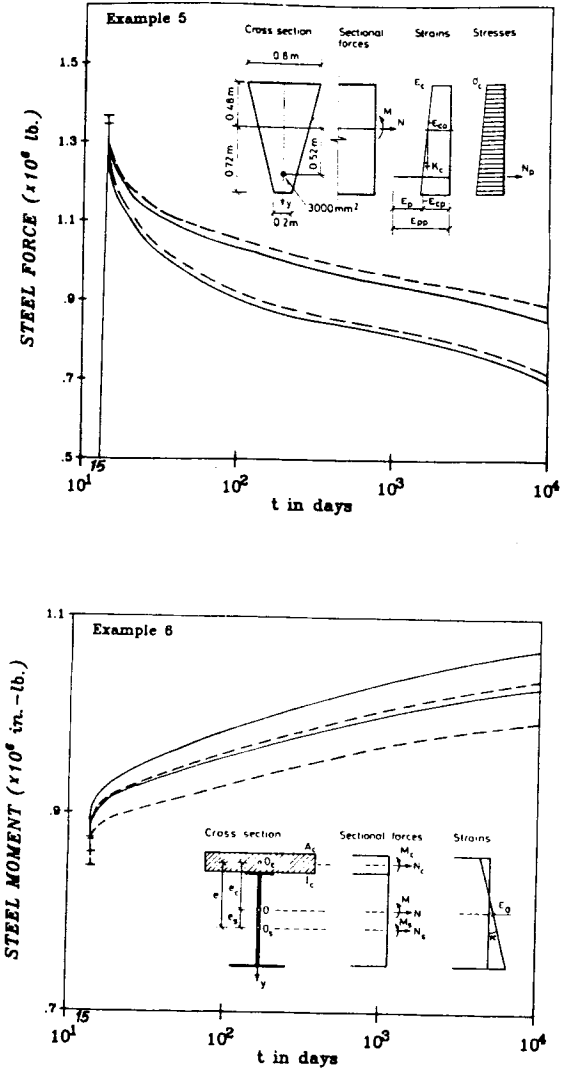


FIG. 15.—Examples 5 and 6 (Same as Fig. 5), by Age-Adjusted Effective Modulus

in which Ψ_4 = an uncertainty factor which has mean value 1 and supplements the uncertainty factors from Eq. 5 (which are all implied in the expressions for E'' , E , ϕ and $\Delta\epsilon_{sh}$); t_0 = age at first loading; $\Delta\epsilon(t) = \epsilon(t) - \epsilon(t_0)$; $\Delta\sigma(t) = \sigma(t) - \sigma(t_0)$; $\Delta\epsilon_{sh}(t) = \epsilon_{sh}(t) - \epsilon_{sh}(t_0)$; $\phi(t, t_0) = E(t_0)J(t, t_0) - 1$ = creep coefficient; and $E''(t, t_0)$ = age-adjusted effective modulus, which may be calculated as

$$E''(t, t_0) = \frac{E(t_0) - R(t, t_0)}{\phi(t, t_0)} \dots \dots \dots (8)$$

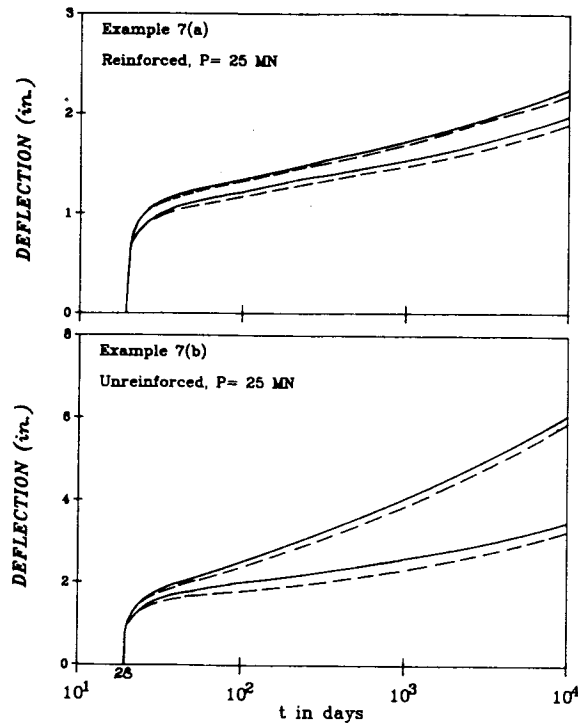
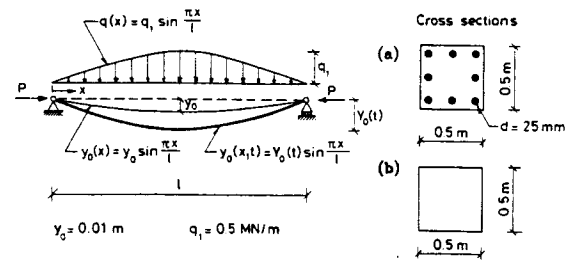


FIG. 16.—Example 7 (Same as Fig. 6), by Age-Adjusted Effective Modulus

Here the relaxation function may be obtained from given $J(t, t')$ either accurately by a step-by-step calculation, as is used in this work (6), or approximately by a simple algebraic formula in Eq. 7.20 of Ref. 6. Eq. 8 may also be alternatively expressed as $E''(t, t_0) = E(t_0)/[1 + \chi(t, t_0)\phi(t, t_0)]$, in which $\chi(t, t_0)$ is called the aging coefficient (and is analogous to a coefficient introduced by Trost on the basis of approximate considerations). Eq. 8 is applicable only for steady loading of the structure.

The method of deterministic calculation of the creep and shrinkage effects for the present examples is described in Ref. 12. The same uncertainty model as before may now be introduced in the calculation of $E''(t, t_0)$, $\phi(t, t_0)$ and $\Delta\epsilon_{sh}(t_0)$, and the latin hypercube sampling may be used again in the same fashion.

The uncertainty factor Ψ_4 describes the errors due to the principle of superposition. Its effect vanishes if $\sigma(t)$ is constant after time t_0 . However, factor Ψ_4 is neglected in the present calculations (i.e., $\Psi_4 = 1$) for the same reasons as before.

The results for the present examples using $N = 16$ are plotted in Figs. 12–16, in which the dashed lines are the values of $\bar{X} \pm \bar{S}$ obtained with the age-adjusted effective modulus, and the solid lines (as in Figs. 2–6) are those obtained with the accurate step-by-step time integration. We see that the age-adjusted effective modulus is generally in close agreement, as previously demonstrated (12) for deterministic solutions.

CONCLUSIONS

1. Compared to the previous solution by two-point estimates of probability moments, the solution based on latin hypercube sampling better captures nonlinear trends and seems more realistic in that the entire range of each random parameter is sampled. It enables a great reduction of computational work if a large number, n , of random parameters for creep and shrinkage is considered. The required number of deterministic structural creep analyses is about $2n$, while for two-point estimates it is 2^n .
2. According to the present numerical results, the probability distribution of the effects of creep and shrinkage is approximately normal (Gaussian) if the random parameters are distributed normally.
3. Consistency of results for an increasing number of samples of random parameters is demonstrated by examples, and the results are close to those obtained before with two-point estimates.
4. A method of taking into account the uncertainty due to the error of the principle of superposition is indicated (Eq. 4).
5. The age-adjusted effective modulus method, which greatly simplified creep structural analysis, may be used for uncertainty analysis of creep and shrinkage effects and yields similar results as accurate step-by-step solutions.

ACKNOWLEDGMENT

Partial financial support under National Science Foundation Grant No. CEE-800 3148 to Northwestern University is gratefully acknowledged.

APPENDIX.—REFERENCES

1. Anderson, C. A., "Numerical Creep Analysis of Structures," *Creep and Shrinkage in Concrete Structures*, Chapter 8, Z. P. Bažant and F. H. Wittmann, eds., John Wiley & Sons, Inc., London, U.K., 1982, pp. 297–301.
2. Anderson, C. A., Whiteman, D. E., Smith, P. D., and Yao, J. T. P., "A Method for Reliability Analysis of Concrete Reactor Vessels," *Publication 78-PVP-100*, ASME, 1979; also *Journal of Pressure Vessels Technology, Transactions of the ASME*, 1979.
3. Bažant, Z. P., "Probabilistic Problems in Prediction of Creep and Shrinkage Effects in Structures," *Proceedings of the 4th International Conference on Application of Statistics and Probability in Soil and Structural Engineering*, Florence, Italy, June, 1983, pp. 325–356.

4. Bažant, Z. P., "Input of Creep and Shrinkage Characteristics for a Structural Analysis Program," *Materials and Structures, Matériaux et Constructions* (RILEM, Paris, France), Vol. 15, No. 88, July–Aug., 1982, pp. 283–290.
5. Bažant, Z. P., "Prediction of Concrete Creep Effects Using Age-Adjusted Effective Modulus Method," *Journal of the American Concrete Institute*, Vol. 69, 1972, pp. 212–217.
6. Bažant, Z. P., "Mathematical Models for Creep and Shrinkage of Concrete," *Creep and Shrinkage of Concrete Structures*, Z. P. Bažant and F. H. Wittmann, eds., John Wiley and Sons, Inc., London, U.K., 1982, pp. 163–256.
7. Bažant, Z. P., and Chern, J. C., "Bayesian Statistical Prediction of Concrete Creep and Shrinkage," *Journal of the American Concrete Institute*, Vol. 81, No. 6, July–Aug., 1984, pp. 319–330.
8. Bažant, Z. P., and Panula, L., "Practical Prediction of Time-Dependent Deformation of Concrete," *Materials and Structures, Matériaux et Constructions* (RILEM, Paris, France), Vol. 11, No. 65, Sept.–Oct., 1978, pp. 307–328; Vol. 11, No. 66, Nov.–Dec., 1978, pp. 415–434; and Vol. 12, No. 69, May–June, 1979, pp. 169–183.
9. Bažant, Z. P., and Panula, L., "Creep and Shrinkage Characterization for Analyzing Prestressed Concrete Structures," *Journal of the Prestressed Concrete Institute*, Vol. 25, No. 3, May–June, 1980, pp. 86–122.
10. Bažant, Z. P., and Panula, L., "New Model for Practical Prediction of Creep and Shrinkage," *American Concrete Institute Special Publication SP-76*, Detroit, Mich., 1982, pp. 7–23.
11. Bažant, Z. P., "Numerical Determination of Long-Range Stress History from Strain History in Concrete," *Materials and Structures—Matériaux et Constructions* (RILEM, Paris, France), Vol. 5, No. 27, May–June, 1972, pp. 135–141.
12. Bažant, Z. P., and Najjar, J., "Comparison of Approximate Linear Methods for Concrete Creep," *Proceedings, ASCE*, Vol. 99, No. ST9, Sept., 1973, pp. 1851–1874.
13. Bažant, Z. P., and Wang, T. S., "Spectral Analysis of Random Shrinkage Stresses in Concrete," *Journal of Engineering Mechanics, ASCE*, Vol. 110, 1984, pp. 173–186; see also *Journal of Structural Engineering, ASCE*, Vol. 110, 1984, pp. 2196–2211.
14. Bethea, R. M., Duran, B. S., and Boullion, T. L., *Statistical Methods for Engineers and Scientists*, Marcel Dekker, Inc., New York, N.Y., 1975, pp. 132–137, 435–440, and 533–557.
15. Çinlar, E., Bažant, Z. P., and Osman, E., "Stochastic Process for Extrapolating Concrete Creep," *Journal of the Engineering Mechanics Division, ASCE*, Vol. 103, 1977, pp. 1069–1088; Discussion, June, 1979, pp. 485–489.
16. Cochran, W. G., and Cox, G. M., *Experimental Design*, John Wiley & Sons, London, U.K., 1950, pp. 103–116.
17. Fisher, R. A., and Yates, F., *Statistical Tables*, 4th ed., Oliver & Boyd, Ltd., Edinburgh, Scotland, 1953.
18. Hald, A., *Statistical Theory with Engineering Applications*, Chapters 16 and 17, John Wiley and Sons, Inc., New York, N.Y., 1952.
19. Madsen, H. O., and Bažant, Z. P., "Uncertainty Analysis of Creep and Shrinkage Effects in Concrete Structures," *Journal of the American Concrete Institute*, Vol. 80, Mar.–Apr., 1983, pp. 116–127.
20. McKay, M. D., *A Method of Analysis for Computer Codes*, Los Alamos National Laboratory, 1980.
21. McKay, M. D., Beckman, R. J., and Conover, W. J., "A Comparison of Three Methods for Selecting Values of Input Variables in the Analysis of Output from a Computer Code," *Technometrics*, Vol. 21, No. 2, May, 1979, pp. 239–245.
22. McKay, M. D., Conover, W. J., and Whiteman, D. C., "Report on the Application of Statistical Techniques to the Analysis of Computer Code," *Report LA-NUREG-6526-MS, NRC-4*, Los Alamos Scientific Laboratory, 1976.
23. "Prediction of Creep, Shrinkage and Temperature Effects on Concrete Structures," *Special Publication SP-76*, American Concrete Institute Committee 209/II, American Concrete Institute, Detroit, Mich., 1982.
24. Raj, D., *Sampling Theory*, McGraw Hill, Inc., pp. 81–84 and 206–209.
25. Steinberg, H. A., "Generalized Quota Sampling," *Nuclear Science and Engineering*, Vol. 15, pp. 142–145.
26. Bažant, Z. P., and Zebich, S., "Statistical Linear Regression Analysis of Prediction Models for Creep and Shrinkage," *Cement and Concrete Research*, Vol. 13, 1983, pp. 869–876.